

ON MICRO-DAMAGE IN HOT METAL WORKING PART 1: EXPERIMENTAL INVESTIGATION

Y. Liu¹), A.D. Foster¹), J. Lin¹),
D.C.J. Farrugia²), T.A. Dean¹)

¹)Department of Manufacturing and Mechanical Engineering
School of Engineering,
University of Birmingham
Edgbaston, Birmingham B15 2TT, UK

²) Corus R, D and T, Swinden Technology Centre
Moorgate, Rotherham, S60 3AR, UK

An experimental programme was defined and performed to investigate the characteristics of micro-damage for a plain CMn and a free machining steel under hot forming conditions. To investigate damage locations – at grain boundaries and around second phase inclusions – a series of constant strain rate tests were carried out on the free machining steel, which contained manganese sulphide inclusions. Specimens from both materials were strained to failure under tension using a Gleeble material simulator at a constant temperature of 1273 K, with strain rates $\dot{\epsilon} = 0.01 - 10 \text{ s}^{-1}$. The damage characteristics of the two different steel microstructures was analysed through microstructural examinations of the tested specimens. Particular attention is focussed on damage locations and features. To investigate the recovery of materials between the intervals of hot deformation, a series of two-step tensile tests were carried out at 1273 K and 10 s^{-1} . The two-step specimens were initially deformed to a strain varying from 0.3–0.7, held for varying recovery periods of 0.3–10 s, then stretched to failure. Flow stress features and strains to failure during the second stage of deformation were analysed with respect to different recovery periods and strain levels at the first stage of deformation. The damage features discovered from the experimentation and microstructural examination provide theoretical evidence to form unified viscoplastic damage constitutive equations for hot forming of free machining steels, which are described in the companion paper.

Key words: Damage, viscoplastic, hot forming, microstructure evolution.

1. INTRODUCTION

Edge cracking occurring in bar/billet, hot-rolled plate and sheet steel is well known within the metal forming industry. Depending on the casting, reheating and thermo-mechanical conditions during rolling, edge or corner cracking is most prominent when rolling low ductility steels (such as free-cutting steels), and

may be dealt with by further rectification processes (e.g. grinding or scrapping), therefore affecting overall product yield.

Corner cracking is intrinsically linked to the as-cast microstructure and cortical zone; the presence of surface and sub-surface defects (oscillation marks); the presence of second phase particles (MnS) in the case of rolling free-cutting steels; and the severity and path of thermo-mechanical conditions. Strain and stress paths with respect to triaxiality and principal longitudinal stresses, together with local temperature gradient due to roll gap conduction heat losses are key parameters affecting the ductility break-up.

It is thought that edge cracking is due to the nucleation, growth and coalescence of micro-damage, the cumulative term for micro-voids and micro-cavities, which are formed by various mechanisms during plastic deformation. Further inward from the visible cracks, the material may still have a high density of micro-damage, which, if over a critical level, can adversely affect the material properties. By modelling the accumulation of damage, it is possible to optimise a rolling schedule to minimise the amount of material containing a high density of damage that must be removed to eliminate defective regions of a product.

The internal deterioration of metals during plastic deformation is significant, or at the least relevant to the manufacture and working life of every metal component. Thus, it is surprising to find that the first detailed study into micro-damage was conducted less than half a century ago. Damage in metals is mainly due to the process of nucleation and growth of micro-cracks and cavities [1, 2]. From the macroscopic perspective, damage has a detrimental influence on the mechanical behaviour of processed metals. Failure, such as internal or external cracking and fracture takes place as a result of damage evolution [3]. From a microscopic viewpoint, damage mechanisms create micro-defects at grain boundaries and within grains and are influenced by thermodynamic conditions and alloying elements within the material [4]. The mechanism of damage evolution is strongly associated with the dominant deformation mechanism at a particular instant.

Ductile damage refers to the initiation and growth of cavities and micro-cracks induced by large plastic deformation in metals [5]. Ductile damage is associated with low temperature cold working and it may be due to debonding of the interface between the matrix and inclusions or second-phase particles, or voids nucleating from other microstructural defects. Voids form at these locations, grow, and eventually link up to form large cracks, leading to ductile fracture [6, 7].

Creep damage refers to the mechanism responsible for the failure of a component held for a period of time under a static stress less than the yield stress of the material. Creep can occur at any temperature [8], but is normally seen at

elevated temperatures [9, 10]. Dominant damage mechanisms under these conditions are due to grain boundary sliding and mobile dislocation multiplication [7]. Cavity nucleation and growth occur at grain boundaries due to grain boundary diffusion, dislocation multiplication and power-law creep of the surrounding matrix [11, 12]. Cavities are often rounded due to the diffusion of material at the grain boundary. Eventually the cavities coalesce to form large cracks and failure occurs [13].

Superplastic damage is associated with fine-grained ($<10\ \mu\text{m}$) materials under superplastic deformation conditions [14–17]. Superplasticity normally occurs at temperatures around and above $T \approx 0.5T_m$ and strain rates of the order $\approx 10e-4\ \text{s}^{-1}$. The dominant deformation mechanisms in superplasticity are grain rotation and grain boundary sliding. This movement requires grains to alter shape as they slide and rotate past each other, this accommodation process is by diffusion and dislocation motion within grains. If the accommodation processes cannot fully provide the required deformation for grains to remain in contact during sliding, the cavities will nucleate. This is largely noted at points of microscopic discontinuity – grain triple points or hard inclusions. Material failure takes place when the cavities coalesce.

Damage in hot forming is associated with high temperatures ($> 0.6T_m$) and high deformation rates, when large deformations are achieved. Damage has been observed at grain boundaries [18] and at interfaces between inclusions and the matrix [19] (referred to as plasticity-induced damage in this paper). Grain boundary damage nucleation, growth and coalescence are by grain boundary sliding [18, 20]. The process of grain boundary migration during recrystallisation can isolate damage formed at an early stage of deformation [21], however smaller grains formed during recrystallisation can exacerbate the grain boundary damage [20]. Grain boundary damage has been found to increase with increasing temperature and decreasing strain rate [18]. Plasticity-induced damage is by void nucleation at inclusion/matrix interfaces which grow and link during deformation [19]. Little work has been done on the interaction of the two dominant damage types in hot deformation.

The objective of the present research is to investigate the effect of microstructure and deformation rates on damage modes and locations in hot deformation. It is intended that the current investigation will aid the construction of a unified phenomenological model of damage and viscoplasticity for the improvement of material modelling in the FE analysis. A group of hot axisymmetric tensile tests and two-step tensile tests were carried out using a Gleeble material simulator. A full set of stress-strain data, along with microstructure analysis, is needed to produce a damage model that is valid over a wide range of conditions. As a part of this, the effect of inclusions and the relationship between grain boundary and plasticity-induced damage is to be clarified.

The work is presented in two papers. The present paper is concerned with the experimental programme conducted to assess the properties of damage associated with the strain rate, material, and recrystallisation and grain size. Experimental stress-strain relationships are analysed and the mechanisms of damage accumulation are obtained from a series of microstructure investigations. The findings of damage mechanisms are summarised. The companion paper uses the knowledge gathered to build a complete set of unified viscoplastic damage constitutive equations, which model the effects of microstructure evolution and strain rate on the accumulation of different types of damage. The model is then determined for a free cutting steel using an EP-based optimisation technique, and validated from experimental data.

2. MATERIAL SELECTION

This study concentrates on the damage properties of a lead-free, free-machining steel. Many high-strength alloys, including free-machining steel, contain hard inclusions that act to block grain movement and deformation. To analyse the effect of inclusions on the dominant damage mechanisms during hot metal forming, a comparison material, plain CMn steel was also tested. The two steels have similar concentrations of carbon, but other element concentrations differ significantly. Notably, the sulphur content was far lower in the manganese steel. Sulphur content for each steel type was: Lead-free 0.287%S; CMn 0.004%S in weight.

A microstructure examination of both steels as supplied has been conducted (Fig. 1). The analysis shows hard particles, mainly of manganese sulphide present within the lead-free machining steel (Fig. 1a). In contrast, the sample of manganese steel contains very few visible hard inclusions (Fig. 1b). At the temperatures used in this experimental programme, the manganese sulphide will have remained as hard inclusions and will not diffuse into the lattice. Further, at elevated temperatures the relative hardness of manganese sulphide increases [22], with the effect that the inclusions deform little during deformation. The examination also revealed the presence of 2-nd phase material in both steel types, which has been removed prior to testing by a soaking process described in the following section.

By choosing the steels described above, the relationship between damage mechanisms and the presence of inclusions can be qualitatively studied whilst concentrating on the damage mechanisms present in a popular steel-type. Tests incorporating an interruption have been carried out using wrought lead-free machining steel, all other tests used the free-cutting steel in as-cast conditions. A comparison of deformation characteristics has been carried out and the steels show similar stress-strain curves.

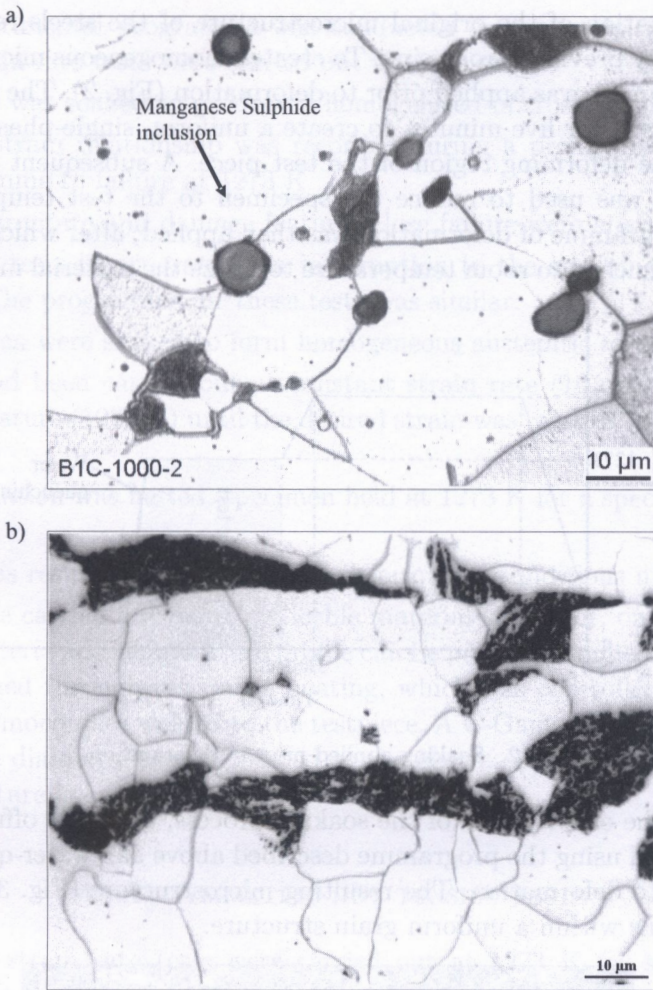


FIG. 1. Original microstructure of the test materials: a) Free machining steel and b) Manganese steel.

3. EXPERIMENTAL PROGRAMME

Hot metal forming relates to forming processes operating in the temperature range $> 0.6T_m$. For steels, a hot rolling temperature of 1273 K is commonplace, and thus has been selected for this study. Strain rates vary over a wide range during multi-pass rolling, especially in hot rolling where cross-section reduction in a single pass is large. In practice, a range of 0.01 s^{-1} to 10 s^{-1} will cover the most essential aspects of strain rate dependence during the initial stage of roughing, and has been chosen for this work.

An examination of the original microstructure of the steels revealed structures created by previous processing. To create a homogeneous microstructure, a soaking programme was applied prior to deformation (Fig. 2). The soak was performed at 1473 K for five minutes to create a uniform, single-phase microstructure within the deforming region of the test piece. A subsequent period of air-cooling (30 s) was used to reduce the specimen to the test temperature. The prescribed programme of deformation was then applied, after which the samples were water-quenched to room temperature to freeze the material microstructure.

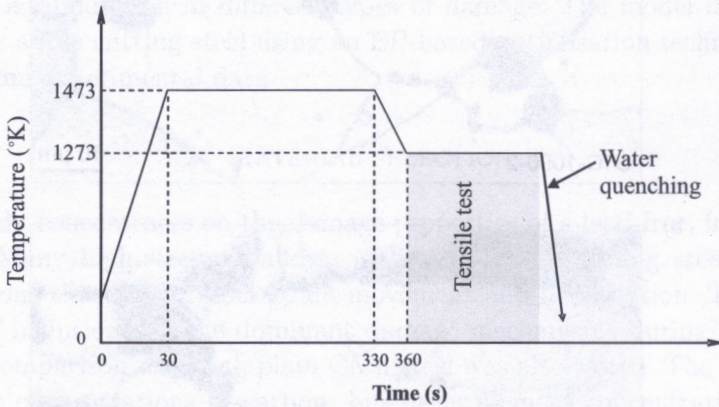


FIG. 2. Soaking applied prior to deformation.

To verify the effectiveness of the soaking process, a sample of free-machining steel was soaked using the programme described above and water-quenched from 1273 K prior to deformation. The resulting microstructure (Fig. 3) shows elongated inclusions within a uniform grain structure.

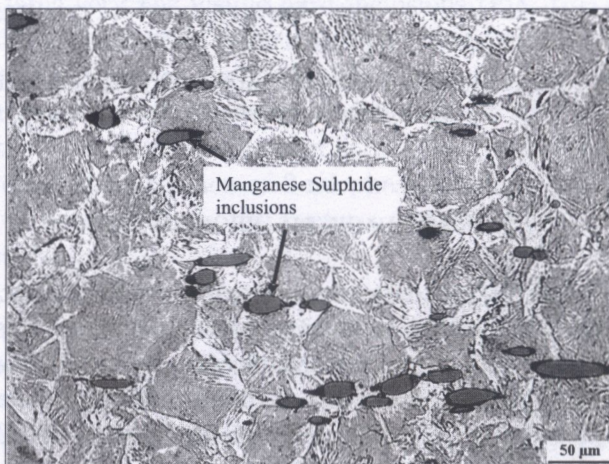


FIG. 3. Microstructure of free machining steel (after soaking) prior to deformation.

The experimental programme was conducted in two parts; firstly a set of constant strain rate tests were carried out in three stages:

1. Sample was soaked to produce a homogenised microstructure
2. Stress-strain relationship was recorded during a pre-defined deformation programme to failure at 1273 K
3. Microstructure and damage features close failure were analysed

Secondly, tests incorporating an interruption to the straining process were performed. The programme for these tests was similar:

1. Specimen were soaked to form homogeneous austenitic microstructure
2. Test had been carried out at constant strain rate (10 s^{-1}) and constant temperature (1273 K) until the desired strain was reached (called interrupt strain)
3. Deformation was halted, specimen held at 1273 K for a specified interrupt period
4. Test was resumed under the same deformation conditions until failure

Tests were carried out using a Gleeble material simulator, on which the deformation criteria and temperature profile can be pre-programmed. Temperature was maintained through resistance heating, which was controlled via feedback from the thermocouples welded to the testpiece. A C-Gauge transducer was used to record the diametral strain, located at the centre of the testpiece where the test temperature is controlled.

4. AXISYMMETRIC HOT TENSILE TESTS

Constant strain rate tests were carried out at 1273 K for strain rates of 0.01 s^{-1} , 0.1 s^{-1} , and 10 s^{-1} and the stress-strain curves for the tests are given in Fig. 4. Certain features can be observed. Under the test conditions, flow-stress initially rises rapidly to a peak value, and peak flow-stress levels are a strong function of strain rate (Fig. 4a). When testing the free-machining steel, peak flow-stress increases as strain rate increases. This can be attributed to a higher level of material hardening occurring during high strain-rate deformation, and less time for the time-dependent material softening processes such as the recovery of dislocations to develop.

Following the peak in flow-stress, the majority of material samples show characteristics attributable to recrystallisation - oscillations in the flow-stress curve are a result of the periodic softening caused by discrete dynamic recrystallisation (DRX) cycles. The softening process produces gradually diminishing undulations in the flow curve until a steady state of hardening due to dislocation accumulation and softening due to DRX and recovery is reached. At this

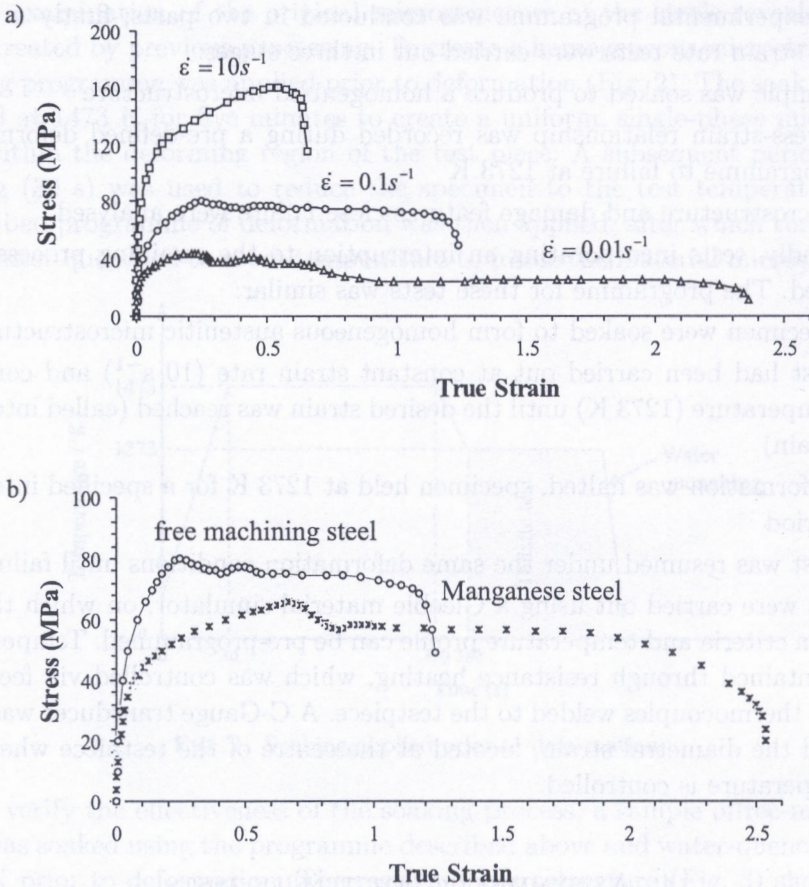


FIG. 4. Stress-Strain curves for a) free machining steel at 1273 K and b) free machining steel and CMn steel at 1273 K and $\dot{\epsilon} = 0.1 \text{ s}^{-1}$.

stage, DRX has become a continuous process and individual cycles can no longer be distinguished. DRX is most prominent at low strain rates owing to the time needed for DRX nucleation sites to grow into recrystallised grains. At high strain rates, no DRX can be seen and the peak in flow strain is followed directly by material failure. Oscillating flow-stress can be observed in manganese steel at a strain rate of 0.1 s^{-1} (Fig. 4b), the amplitude of the second peak is much lower than the first one suggesting a tendency towards a steady state of continuous DRX.

With all specimens, damage eventually reaches a critical level within the material and starts to coalesce. This is reflected in the stress-strain plot by a rapid reduction in flow-stress leading to failure. Strain to failure is inversely related

to the strain rate and peak flow-stress, suggesting that damage accumulation is affected by the mechanisms that allow plastic deformation - grain boundary sliding and mobile dislocations. The long steady period of straining observed at 0.01 s^{-1} suggests that the effects of DRX act to retard the accumulation of damage in hot deformation. Manganese steel, which has no inclusions, has a higher ductility than the lead-free machining steel (Fig. 4b) suggesting that the inclusions increase the accumulation or coalescence of damage in hot deformation.

Water quenched test pieces were polished and etched close to the site of fracture, to allow damage mechanisms to be studied. Microstructures were examined normal to the fracture plane of the test piece. A representative selection of regions showing particular features can be seen in Fig. 5. Plasticity-induced damage (Fig. 5a) is observed around inclusions within the matrix. Characteristic oval voids surrounding central inclusions can be seen. Under these conditions, deformation occurs by plastic deformation of grains, and not by grain rotation and grain boundary sliding, thus almost no damage is observed at the grain boundaries. In addition to plasticity-induced damage, grain boundary damage (Fig. 5b) can be seen in various forms at low strain-rate deformation ($\dot{\epsilon} = 0.01 \text{ s}^{-1}$) as cracks along grain boundaries (feature A) and as voids at triple points of grains (feature B). Grain boundary damage becomes prominent in test pieces deformed at low values of the strain-rate, in conditions that favour deformation by movement of adjacent grains and in which DRX reduces grain size, encouraging the aforementioned mechanism. Voids are most prominent at triple points, for the same reason as that in superplastic damage. The triple points are points of large geometric discontinuity and thus they require the most accommodation by sub-granular deformation.

The microstructure examinations support the initial theory that two damage mechanisms exist, and often coexist during the hot, high strain rate deformation of steels. Plasticity-induced damage is characterised by void growth around debonded inclusion/matrix interfaces. Dislocations multiply around the inclusion, eventually destroying the bonding at the interface. Growth is increased due to the stress concentration produced around the void, causing the void to propagate through the grain. Plasticity-induced damage is encouraged during low temperature, high strain rate deformation, where most plastic deformation is accommodated by changes in grain shape. The extent of plasticity-induced damage is directly related to the distribution density of inclusions within the metal. Grain boundary damage is characterised by voids at triple points of grains, and cracks along grain boundaries. Cavities at triple points between grains are formed from the movement and rotation of neighbouring grains. Cracks along grain boundaries can be nucleated by grain boundary sliding or by a build up of dislocations at grain boundaries.

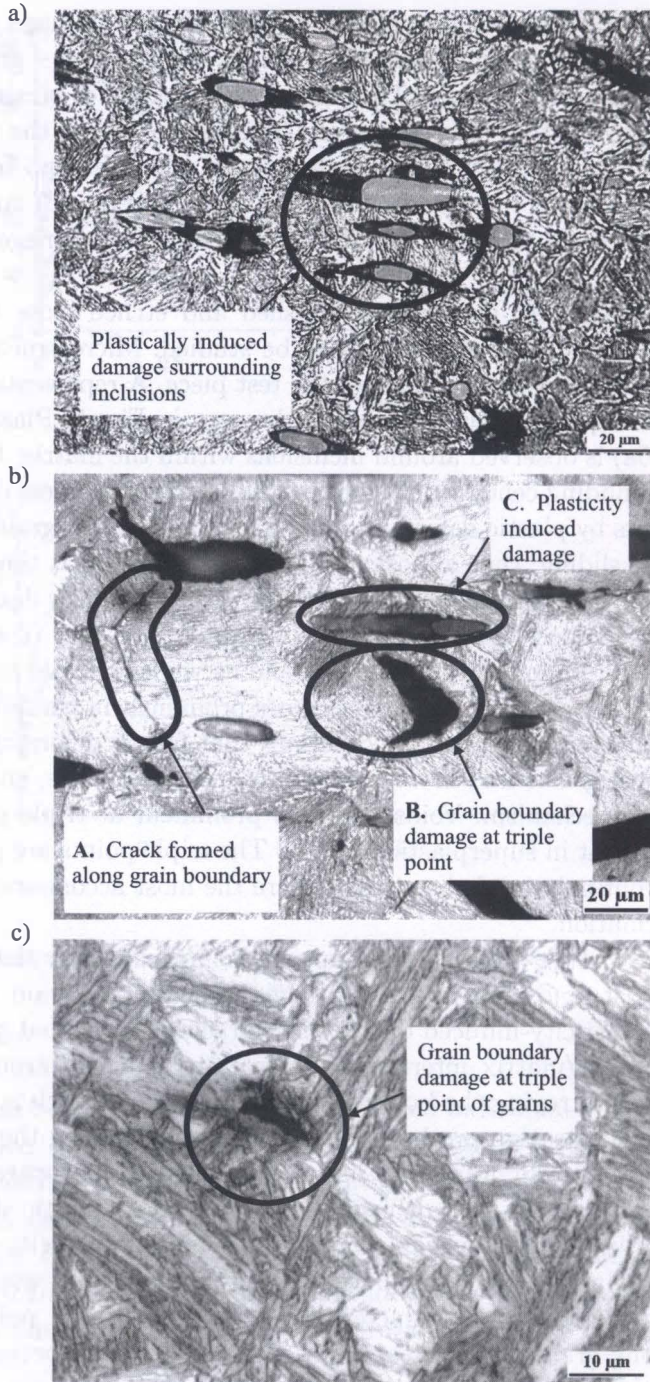


FIG. 5. Damage features of tested samples close to failure. a) free-machining steel at $\dot{\epsilon} = 10 \text{ s}^{-1}$, b) free-machining at $\dot{\epsilon} = 0.01 \text{ s}^{-1}$, and c) CMn steel at $\dot{\epsilon} = 0.01 \text{ s}^{-1}$.

Manganese steel microstructures reveal grain boundary damage at triple points, similar to that found in the free-machining steel samples. Figure 5c shows a typical example of grain boundary damage at triple points on a specimen deformed at 1273 K and a strain rate of 0.01 s^{-1} . Plasticity-induced damage forms around the inclusions, the manganese steel contains few inclusions, and so there is no plasticity-induced damage in the steel. As such, it can be concluded that plasticity-induced damage is a feature of steels with a high number of inclusions and that inclusions play an important role in the mechanism of damage development in hot forming. It is also speculated that inclusions may encourage grain boundary damage, as they block mobile dislocations, increasing grain hardness with the effect of encouraging grain boundary movement. In addition to this, inclusions block the migrating boundaries, creating boundaries that do not move and thus are prone to the build-up of damage.

Figure 5b shows both the grain boundary damage and plastically induced damage present within the same sample. For high strain rate, and high temperature conditions there is no clear definition as to which damage mechanism will be dominant. Micrograph results analysed from this experimental programme suggest that two damage mechanisms often coexist, both contributing to the degradation of the material microstructure and with no clear dominant mechanism. It is believed that this transition phase between dominant damage types has not been fully recognised until now.

5. INTERRUPTED AXISYMMETRIC HOT TENSILE TESTS

Damage formation is a continuous process and accumulates during all stages of deformation. A specimen that has been pre-strained may exhibit damage properties related to its strain history on the application of further straining, due to the presence of small voids formed during the initial deformation. As a result, the strain to failure of the reloaded specimen will be reduced from that of a specimen with no strain history as damage will coalesce at lower strains leading to premature failure. Research has shown that under certain conditions, for instance under certain stress state conditions, if the initial strain is low, damage will heal if deformation is stopped and sufficient time is given for recovery to take place [23].

The formation of damage at low strains has been identified in a testpiece of free-machining steel deformed at 0.01 s^{-1} and quenched once a strain of 0.3 had been achieved (Fig. 6). Some damage at grain boundaries is already apparent, confirming that damage accumulation is gradual and takes place throughout deformation. An experimental programme has been conducted to record the effects of pre-straining on the characteristics of a testpiece during subsequent deformation. It is hypothesised that two forms of damage healing may occur following

a stress relaxation: firstly, if a stress is removed and material surrounding a crack has been only elastically deformed, the crack will close. Under certain circumstances, for example a recrystallisation front passing over the crack, the damage may heal completely. Secondly, if a grain boundary migrates over an area containing small voids, the voids may become locked inside the grains, where stress will be dispersed around the matrix discontinuity.

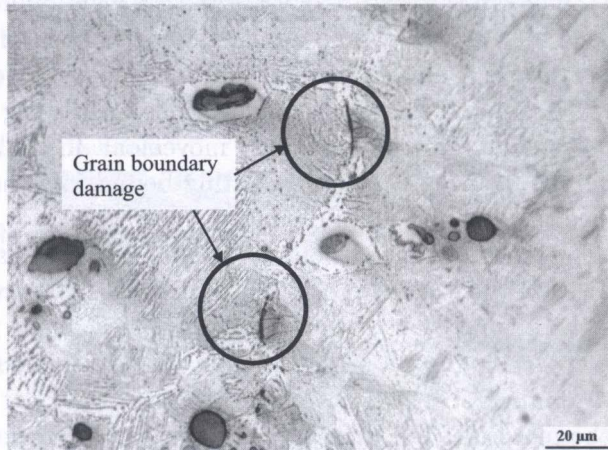


FIG. 6. Free-machining steel strained to 0.3 at 1273 K at $\dot{\epsilon} = 0.01 \text{ s}^{-1}$.

Figure 7 shows a comparison of four stress-strain curves obtained by reloading following an interruption to deformation. Testpieces were strained at $\dot{\epsilon} = 10 \text{ s}^{-1}$ at 1273 K to strains about 0.3 to 0.68 before being held at 1273 K for 1 s and 2 s intervals. Deformation was then restarted at $\dot{\epsilon} = 10 \text{ s}^{-1}$ and 1273 K. The strain at which the interrupt is initiated clearly affects the strain-to-failure on reloading, from which it is concluded that material characteristics are strongly influenced by the strain history. It can be seen that a specimen that has experienced a large amount of strain will be permanently weakened. Further to this, the greater the strain preceding an interruption, the faster damage will coalesce on further strains being applied. The tests shown in Fig. 7 exhibit similar stress-strain curves before reaching a peak-stress value, after which the characteristic stress reduction associated with the coalescence of micro-damage leads to failure. However it is important to realise that time-dependent annealing mechanisms will be taking place during the interrupt time between the periods of constant strain rate deformation which will affect the ductility characteristics. During the interrupt time the metadynamic recrystallisation (MDRX) and static RX (SRX), recovery and grain growth mechanisms will alter the grain size and dislocation density of the specimen [24], all of which affect the ductility properties of a specimen on reloading.

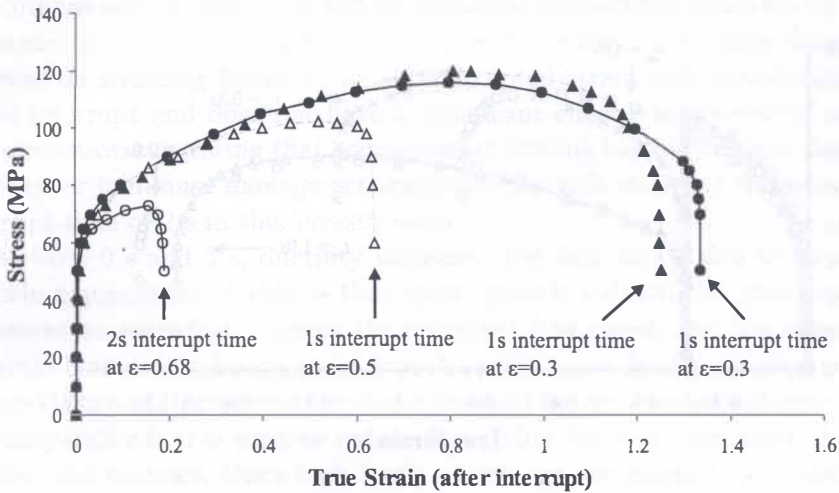


FIG. 7. Flow-stress on reloading after an interruption period.

To analyse the effect of MDRX and other metadynamic processes on damage, further tests were performed with interrupt periods of 0.3, 1, 2, 3, 5, and 10 s. Figure 8 summarises the results of all tests performed with an interrupt strain of approximately 0.3. Figure 8a shows interrupt times of 0–2 s. For very short interruption times, peak flow-stress on reloading increases. After this, the trend is reversed – as interrupt time increases strain at fracture increases and peak flow-stress decreases – the material has greater ductility. Figure 8b shows interrupt times of 2–10 s. At these times, the trend is reversed once again. Longer interrupt times create a less ductile material with higher peak flow-stress and lower strain at fracture. Peak flow-stress and strain at failure are plotted in Fig. 8c. The pattern of initial decrease in ductility, followed by an increase in ductility before returning to decreasing ductility can be explained by MDRX.

DRX is triggered once a critical dislocation density is reached [25]. At this point new grains are nucleated at the grain boundaries. Nucleation points do not immediately grow, and their growth rate is restricted by high strain rates. Thus, a sample may show no macrosigns of recrystallisation, but may have a population of nucleation points within it. If deformation is stopped, the nucleations can develop into new grains, causing MDRX to occur [26]. Once MDRX is complete, the grain size will be smaller, increasing ductility. If left, normal grain growth will occur (as large grains have a lower energy state) increasing the grain size, lowering ductility, and increasing flow stress on reloading. Thus, it is proposed that at times between 0–0.3 s, the nucleated grains are growing but are small and grain growth of large grains is dominant, from 0.3–2 s MDRX it takes place

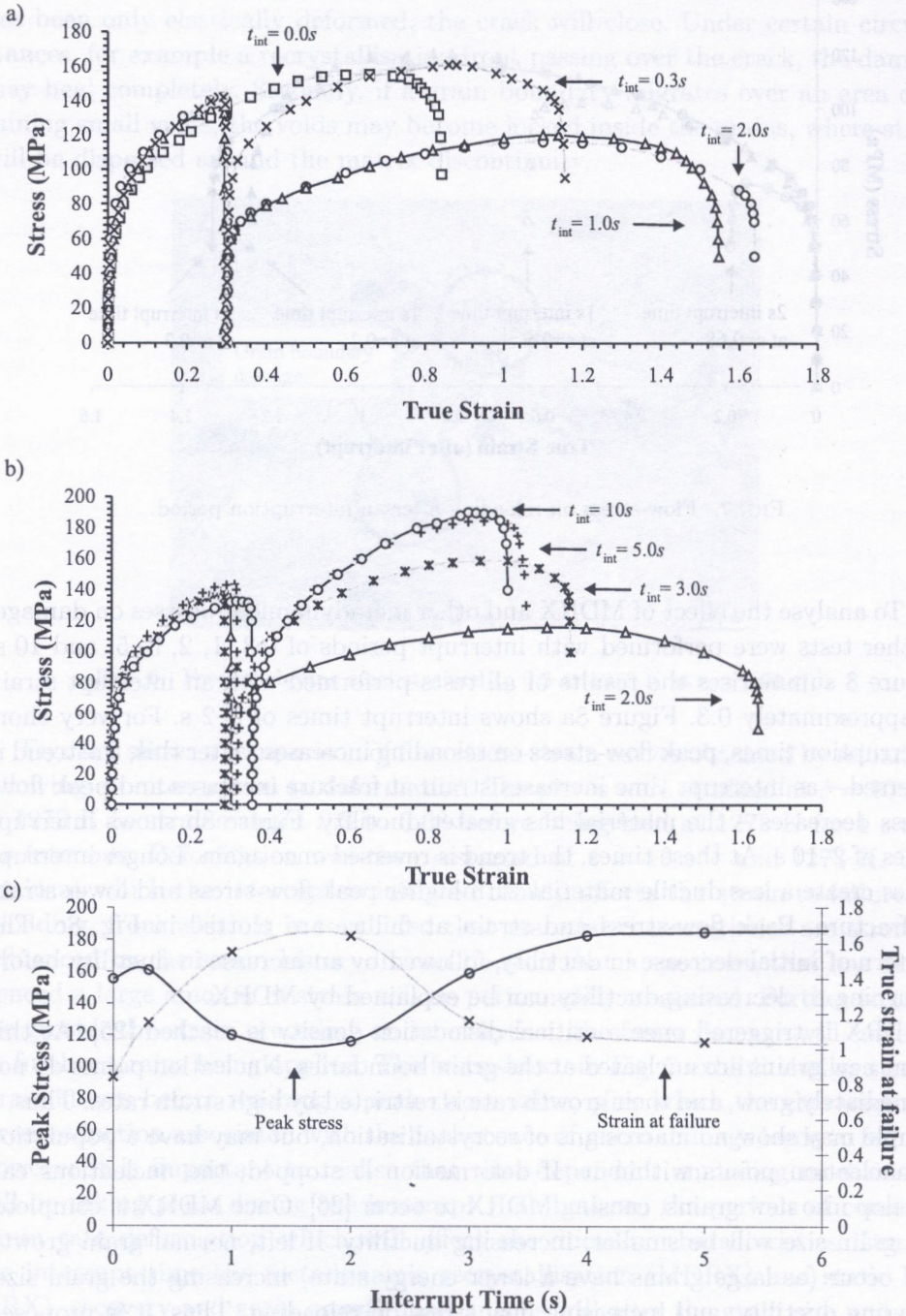


FIG. 8. Interrupted tests. a) Interruption time 0–2 s, b) interruption time 2–10 s, and c) summary of reloading properties.

reducing the average grain size and annihilating dislocations, and from 2 s onward the static grain growth occurs creating larger grains. The large deformation achieved on straining following a low interrupted strain indicates damage prior to the interrupt and does not have a significant effect on subsequent reloading characteristics, suggesting that some damage healing has taken place. Maximum ductility, or minimum damage accumulation per unit strain, is reached with an interrupt time of 2 s in this investigation.

Between 0 s and 3 s, ductility increases, but flow stress also increases. One possible explanation of this is that grain growth reduces the grain boundary movement on reloading, causing the increased flow stress, and the migration of the grain boundaries during grain growth causes some damage healing (an effect discussed earlier), increasing the strain reached before damage coalesces.

Recrystallisation is seen to reduce the ability for small amounts of damage to grow and coalesce. Once high levels of damage are reached, recrystallisation and recovery can no longer affect the coalescence of damage, and the material has poor mechanical properties. The reduced grain size following recrystallisation will increase ductility and reduce the buildup of both damage types. Small grains can slide and rotate around each other with greater ease, thus reducing the grain boundary damage. In turn, plastic deformation becomes increasing by grain boundary sliding, reducing plastic strain by dislocation motion and thus reducing the plasticity-induced damage. Inclusions significantly improve the machining properties of the steel, however the same inclusions increase the micro-damage created during hot forming, which - if not - controlled can reduce mechanical performance.

6. CONCLUSIONS

The experimental programme gives convincing evidence that failure of steel under hot, high strain-rate deformation can occur by plasticity-induced damage, grain boundary damage, or a combination of both, depending on the rate of deformation and the microstructure of the material. High strain rates have been shown to encourage the plasticity-induced damage, and low strain rates to favour the grain boundary damage. Changes to the material microstructure can be used to delay the onset of damage, for instance reduction the grain size is shown to increase the strain at failure. It is suggested that this is because the nucleation and growth of both damage mechanisms are proportional to the grain size, thus small grains are associated with high ductility. Inclusions are shown to encourage plasticity-induced damage, and it is speculated that they also indirectly encourage the grain boundary damage.

Interrupted tensile tests show that damage is a strong function of the strain history, and once a specimen has accumulated too much damage, it is perma-

nently weakened. Recrystallisation results in some damage healing, so long as damage levels are low.

Further research is needed to clarify the effect of recrystallisation on both plasticity-induced and grain-boundary damage mechanisms. Damage healing during strain reversal under hot conditions is also an interesting area that is still in its infancy, as is the effect of complex stress states on damage.

ACKNOWLEDGMENTS

The financial support provided by Corus UK Ltd for both Y. Liu and A. D. Foster is gratefully acknowledged.

REFERENCES

1. L. ENGL H. KLINGELE, *An atlas of metal damage*, Wolfe Publishing Ltd, London, UK, 1981.
2. J. L. CHABOCHE, *Continuum damage mechanics: Present state and future trends*, Nuclear Eng. and Design **105**, 19–33, 1987.
3. D. KRAJGINOVIC, *Damage mechanics: accomplishments, trends and needs*, International Journal of Solids and Structures, **37**, 267–277, 2000.
4. J. LEMAITRE, *Continuous damage mechanics model for ductile fracture*, J. Eng. Mat. Technol., **107**, 83–89, 1985.
5. J. LEMAITRE, *How to use damage mechanics*, Nuclear Engineering and Design, **80**, 233–245, 1984.
6. P. F. THOMASON, *Ductile fracture of metals*, Publishers: Pergamon Press, Oxford 1990.
7. V. TVERGAARD, *Material failure by void growth to Coalescence*, Adv. App. Mech, **27**, 83–151, 1990.
8. F. W. BRUST and B. N. LEIS, *A new model for characterising primary creep damage*, Int. J. Fract., **54**, 45–63, 1992.
9. D. MCLEAN, *Mechanical properties of metals*, Publishers: Wiley, ISBN 0471585572, 1962.
10. H. J. FROST and M. F. ASHBY, *Deformation-mechanism maps*, Publishers: Pergamon Press Oxford, 1982.
11. B. F. DYSON *et al.*, *The influence of stress state on creep resistance: Experimentation and modelling*, Acta Met. **29**, 1573–1580, 1981.
12. M. F. ASHBY and B. F. DYSON, *Creep damage mechanics and micro-mechanisms*, National physical laboratory, 1984
13. A. C. F. COCKS and M. F. ASHBY, *On creep fracture by void growth*, Progress in Mat. Sci. **27**, 189–244, 1982.
14. J. LIN and Y. LIU, *Development of unified constitutive equations for modelling microstructure evolution in hot deformation*, Proceedings of the international conference

on advanced materials processing technologies, Madrid, Spain [AMPT'01], 2, 883–890, 2001.

15. Z. DU and S. WU, *Kinetic equation for damage during superplastic deformation*, J. of Mat. Proc. Tech. **52**, 270–279, 1995.
16. H. L. XING and Z. R. WANG, *Prediction and control of cavity growth during superplastic sheet forming with finite-element modelling*, J. of Mat. Proc. Tech. **75**, 87–93, 1998.
17. M. LAGOS, *Elastic instability of grain boundaries and the physical origin of superplasticity*, Physical review letters, **85**, 2332–2335, 2000.
18. F. E. WHITE and C. ROSSARD, *A mechanism for the fracture of steel in high temperature torsion and its relation to structural changes*, [in:] Deformation under hot working conditions, Iron and Steel Inst. UK, 14–21, 1968.
19. A. NICHOLSON *et al.*, *Hot workability testing at united steel companies*, [in:] Deformation under hot working conditions, Iron and Steel Inst. UK, 161–167, 1968.
20. R. J. DIMELFI, *Grain boundary sliding and its relation to ductility and fracture in fine-grained polycrystalline materials with a particular focus on γ -TiAl*, Materials Science and Engineering A, **237**, 141–149, 1997.
21. B. MINZ *et al.*, *Hot ductility of steels and its relationship to the problem of transverse cracking during continuous casting*, International Materials Review **36**, 187–217, 1991.
22. R. HONEYCOMBE, H. BHADESHIA, *Steels*, Publishers: Edward Arnold, London 1995.
23. A. A. BOGATOV, *The mechanics of the ductile damage under the metal forming*, 6-th Int. ESAFORM conf. on Mat. Forming, 2003.
24. F. GAO *et al.*, *Thermodynamic study of the critical nucleus size for metadynamic recrystallisation*, Materials Science & Engineering A, **277**, 33–37, 2000.
25. J. LIN, Y. LIU, *A set of unified constitutive equations for modelling microstructure evolution in hot deformation*, J. of Mat. Pro. Tech., **143-144**, 281–285, 2003.
26. P. URANGA *et al.*, *Transition between static and metadynamic recrystallization kinetics in coarse Nb microalloyed austenite*, Materials Science & Engineering A, **345**, 319–327 2003.

Received August 18, 2005; revised version January 16, 2006.
